Experimental Hematology

Experimental Hematology 2019;69:37–42

Distinct pathways affected by menin versus MLL1/MLL2 in *MLL*-rearranged acute myeloid leukemia

Yufei Chen[a], Kenneth L. Jones[a], Konstantinos Anastassiadis[b], Andrea Kranz[b], A. Francis Stewart[b], Jolanta Grembecka[c], Matthew Meyerson[d], and Patricia Ernst[a,e]

[a]*Department of Pediatrics, University of Colorado, Denver/Anschutz Medical Campus. Aurora, CO, USA;* [b]*Genomics and Stem Cell Engineering, Biotechnology Center, Technische Universität Dresden, Dresden, Germany;* [c]*Department of Pathology, University of Michigan, Ann Arbor, MI, USA;* [d]*Department of Medical Oncology, Dana-Farber Cancer Institute, Boston, MA, USA;* [e]*Department of Pharmacology, University of Colorado, Denver/Anschutz Medical Campus. Aurora, CO, USA*

(Received 18 September 2018; revised 5 October 2018; accepted 6 October 2018)

Disrupting the protein–protein interaction for molecularly targeted cancer therapeutics can be a challenging but promising strategy. Compounds that disrupt the interaction between menin, a chromatin-binding protein, and oncogenic mixed lineage leukemia fusion proteins (MLL-FPs) have shown significant promise in preclinical models of leukemia and have a high degree of selectivity for leukemia versus normal hematopoietic cells. Biochemical and structural studies demonstrate that, in addition to disrupting the menin–MLL-FP interaction, such compounds also inhibit menin–MLL1, menin–MLL2, and other menin-interacting proteins. Here, we address the degree to which disruption of menin–MLL-FP interactions or menin–MLL1/MLL2 interactions contribute to the antileukemia effect of menin inhibition. We show that *Men1* deletion in MLL-AF9-transformed leukemia cells produces distinct cellular and molecular consequences compared with *Mll1;Mll2* co-deletion and that compounds disrupting menin–MLL N-terminal interactions largely phenocopy menin loss. Moreover, we show that *Mll1;Mll2*-deficient leukemia cells exhibit enhanced sensitivity to menin interaction inhibitors, which is consistent with each regulating complementary genetic pathways. These data illustrate the heightened dependency of MLL-FPs on menin compared with wild-type MLL1/MLL2 for regulation of downstream target genes and argue that the predominant action of menin inhibitory compounds is through direct inhibition of MLL-FPs without significant contribution from MLL1/MLL2 inhibition.

Patients with chromosomal translocations involving the *Mixed Lineage Leukemia 1* gene (*MLL, MLL1, KMT2A*) represent an exception to overall favorable outcomes for children with acute leukemia [1]. Menin, which is encoded by the *Men1* gene, is a tumor suppressor in neuroendocrine tissues but is essential for MLL1 fusion oncoprotein (MLL-FP)-mediated leukemogenesis. MLL-FP binding to menin bridges an interaction with Lens Epithelium-Derived Growth Factor (LEDGF), which in turn binds histone H3 dimethyl lysine 36 (H3K36me2)-modified chromatin [2,3]. Menin also interacts with endogenous wild-type MLL1 and MLL2 [2,4,5] with quantitative proteomics indicating nearly 1:1 stoichiometry of menin with MLL1 and MLL2 complexes [6]. Because of the essential nature of the menin/LEDGF interaction for MLL-FPs to target to chromatin, small-molecule inhibitors have been developed that disrupt menin binding to the N-terminus of MLL-FPs [7–11]. Menin binds to MLL-FPs, MLL1, MLL2, and other proteins using the same pocket, so small-molecule inhibitors may disrupt all of these interactions in cells. To clarify through which pathways inhibitors of the menin–MLL N-terminus act, we compared cellular and molecular alterations in in MLL-AF9-transformed leukemia cells using

YC's present address: Seattle Genetics, Inc., Bothell, WA, USA.

Offprint requests to: Dr. Patricia Ernst, Department of Pediatrics, University of Colorado Anschutz Medical Campus, 12800 E. 19th Ave., Mail Stop 8302, Room P18-4117, Aurora, CO 80045; E-mail: patricia.ernst@ucdenver.edu

Supplementary data related to this article can be found online at https://doi.org/10.1016/j.exphem.2018.10.001.

https://doi.org/10.1016/j.exphem.2018.10.001

genetic and pharmacologic manipulation of *menin*, *Mll1*, and *Mll2*.

Methods

Mice and generation of MLL-AF9-transformed cells

$Lin^-/Sca\text{-}1^+/c\text{-}Kit^+$ (LSK) or $c\text{-}Kit^+$ cells were sorted from $Cre{:}ER^{T2}{;}Mll1^{F/F}{;}Mll2^{F/F}$ and $Cre{:}ER^{T2}{;}Men1^{F/F}$ mice and transduced with MSCV-MLL-AF9-YFP or MSCV-MLL-AF9-GFP (gifts from Drs. Scott Armstrong and Mick Milsom) as described previously [12]. Transduced cells were replated in M3434 medium (StemCell Technologies) for more than four rounds to generate transformed cells.

Quantitative real-time polymerase chain reaction

Quantitative real-time polymerase chain reaction (qRT-PCR) procedures were as described previously [12] using the TaqMan Gene Expression Master Mix (Applied Biosystems) assays or primers as follows: *Magohb*: Applied Biosystems Mm01200054_m1; *Mef2c*: Applied Biosystems Mm01340842_m1; *Gapdh*: Applied Biosystems 4308313; *Meis1*: GAGCAAGGTGATGGCTTGGA and TGTCCTTATCAGGGTCATCATCG; *Meis1* Probe: AACAGTGTAGCTTCCCCCAGCACAGGT. The following primer pairs were fused with SYBR Green Supermix (Bio-Rad): *Pigp*: TGCCCGTCTACCTCCTTATC and ATGGGGACATCTCTCAATGC. *Jmjd1c*: CACATTCTTGGATCTGTGACCA and ATGCTGTCTTTGCAGTTGAGG. *Cdkn2c*: AACCATCCCAGTCCTTCTGTCA and CCCCTTTCCTTTGCTCCT AATC. *Il3ra*: CTGGCATCCCACTCTTCAGAT and GGTC CCAGCTCAGTGTGTA.

RNA-sequencing and genomic analyses

RNA-sequencing (RNA-seq) and Gene Set Enrichment Analysis (GSEA) were performed as described previously [12] and the gene lists represented in the Venn diagrams and supplemental files represent data filtered for greater than twofold change and $p < 0.05$. Diagrams and overlap lists were generated using BioVenn [13]. The RNA-seq data reported here have been deposited at the National Center for Biotechnology Information Gene Expression Omnibus with the accession code GSE117933.

Cell proliferation and viability assays

Proliferation was assessed by bromodeoxyuridine (BrdU) incorporation according to the manufacturer's protocol using the allophycocyanin (APC) BrdU Flow Kit (BD Biosciences) with a 30-minute incubation with BrdU. Cell viability was determined by propidium iodide (PI, Sigma-Aldrich) and Annexin V-APC (BioLegend) staining. Cre induction in leukemia cells was initiated in culture medium supplemented with 100 nmol/L 4-OHT (Sigma-Aldrich). After 24 hours, 4-OHT was removed by exchanging the medium and cells were cultured for the times indicated in the figure legends. Both MI-2 (Cayman) and MI-2-2 were dissolved in dimethylsulfoxide. Three thousand cells in 200 μL were treated with MI-2 or MI-2-2 for 3 days.

Chemistry

Chemical synthesis and chemical characterization of MI-2 and MI-2-2 compounds have been described previously [9,10].

Results and discussion

We recently showed that co-deletion of *Mll1* and *Mll2* in MLL-FP-transformed leukemia inhibited cell growth through modulation of several leukemia survival pathways [12]. MLL-FPs have also been shown to directly regulate anti-apoptotic survival pathways [14]. To deconvolute the contributions of MLL-FP versus MLL1/MLL2 inhibition that would occur with menin inhibitors, we compared the effect of deleting *Men1* with that of co-deletion of *Mll1* and *Mll2*. We selected the time points for analysis based on complete gene deletion and loss of the corresponding transcript (observed by 48 hours, Supplementary Figure E1A, online only, available at www.exphem.org). A severe reduction in S-phase cells was observed 5 days after initiating *Men1* deletion (from 56% to 16%) concomitant with a G_0/G_1 accumulation (Figures 1A and 1B). In contrast, *Mll1;Mll2* deletion resulted in milder reduction in S-phase cells (from 56% to 32%) and much larger accumulation of sub-G_0/G_1 cells. The selective effect on cell cycle may be due to the fact that *Men1* deletion affects expression of the cyclin-dependent kinases CDK4 and CDK6 and *Mll1;Mll2* deletion does not (Figures 1A and 1B, Supplementary Figure E1B, online only, available at www.exphem.org). *Mll1;Mll2*-deleted cells exhibited increased Annexin V binding and PI permeability at day 3, which accumulated over time (Figure 1C and data not shown), suggesting that cell death plays a larger role in the growth inhibition observed upon co-deletion of *Mll1* and *Mll2* [12]. To broadly compare the molecular characteristics of *Men1* versus *Mll1;Mll2* deficiency, we performed side-by-side RNA-seq analysis in MLL-AF9-transformed cells at day 3 prior to the execution of cell cycle/cell death phenotypes. *Men1* deletion resulted in both upregulated and downregulated genes (366 and 347 genes, respectively, Figure 1D and Supplemental Table E1, online only, available at www.exphem.org), whereas *Mll1;Mll2* deletion resulted in fewer changes using the same criteria for data analysis (70 upregulated and 194 downregulated, Figure 1D). Comparison of *Men1*- versus *Mll1;Mll2*-deregulated genes showed minimal overlap of differentially expressed genes; only 12% of the downregulated genes and 7% of the upregulated genes in *Men1*-deficient leukemia cells were shared with *Mll1;Mll2*-deficient cells (Figure 1D). We performed qRT-PCR validation in MLL-AF9 cells focusing on MLL-FP-regulated genes or those unique to the MLL1/MLL2-regulated pathways [12,15]. The MLL-FP targets *Meis1* and *Jmjd1c*

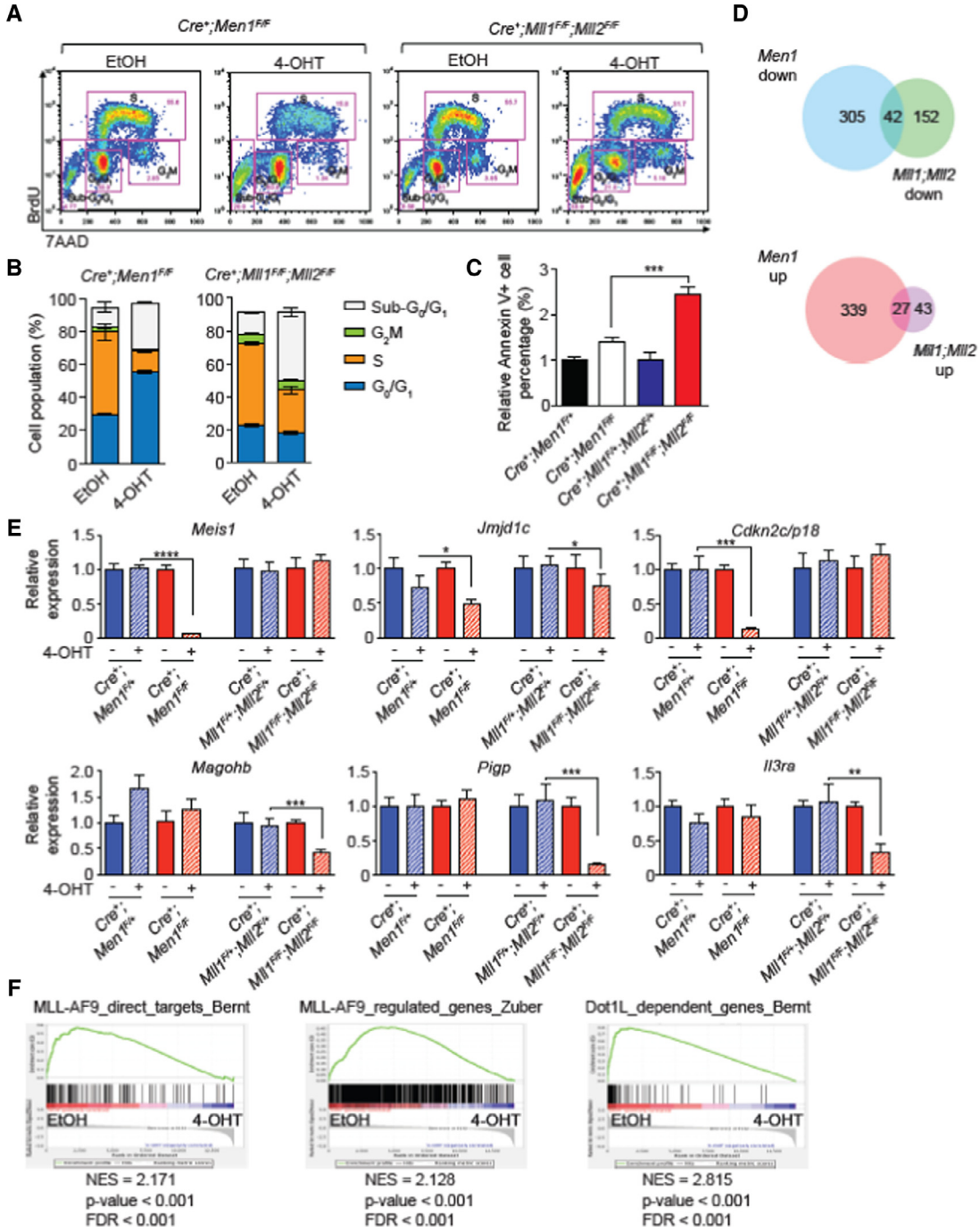

Figure 1. Loss of *Men1* versus *Mll1;Mll2* shows different cellular and molecular effects in MLL-AF9-transformed cells. **(A,B)** Representative FACS plots **(A)** and quantification **(B)** showing BrdU incorporation and DNA content in *Men1*- and *Mll1;Mll2*-deficient MLL-AF9 cells. MLL-AF9-transformed cells were treated with ethanol or 4-OHT for 24 hours to induce the deletion of *Men1* or *Mll1;Mll2*. After an additional 4 days, cells were incubated with BrdU for 30 minutes and were processed to detect BrdU and DNA content by flow cytometry. The apoptotic sub-G_0/G_1, G_2M, S, and G_0/G_1 gates are shown. **(C)** Relative Annexin V^+ cell percentage compared with control cells 3 days after initiating gene deletion. **(D)** Venn diagram showing the overlap of downregulated and upregulated genes with *Men1* and *Mll1;Mll2* deletion. Differentially expressed genes (Supplementary Table E1, online only, available at www.exphem.org) were identified as described in the Methods. **(E)** qRT-PCR of select genes after *Men1* or *Mll1;Mll2* deletion in MLL-AF9-transformed cells. Gene expression was determined 3 days after initiating gene deletion. Data are represented as averages ± standard deviation (SD). *$p < 0.05$; **$p < 0.01$; ***$p < 0.001$; ****$p < 0.0001$. One representative experiment of five is shown. **(F)** GSEA plots showing enrichment of MLL-AF9 direct binding targets or Dot1L-dependent genes [16] and MLL-AF9-regulated genes [15] in *Men1*-deficient (4-OHT) MLL-AF9-transformed cells.

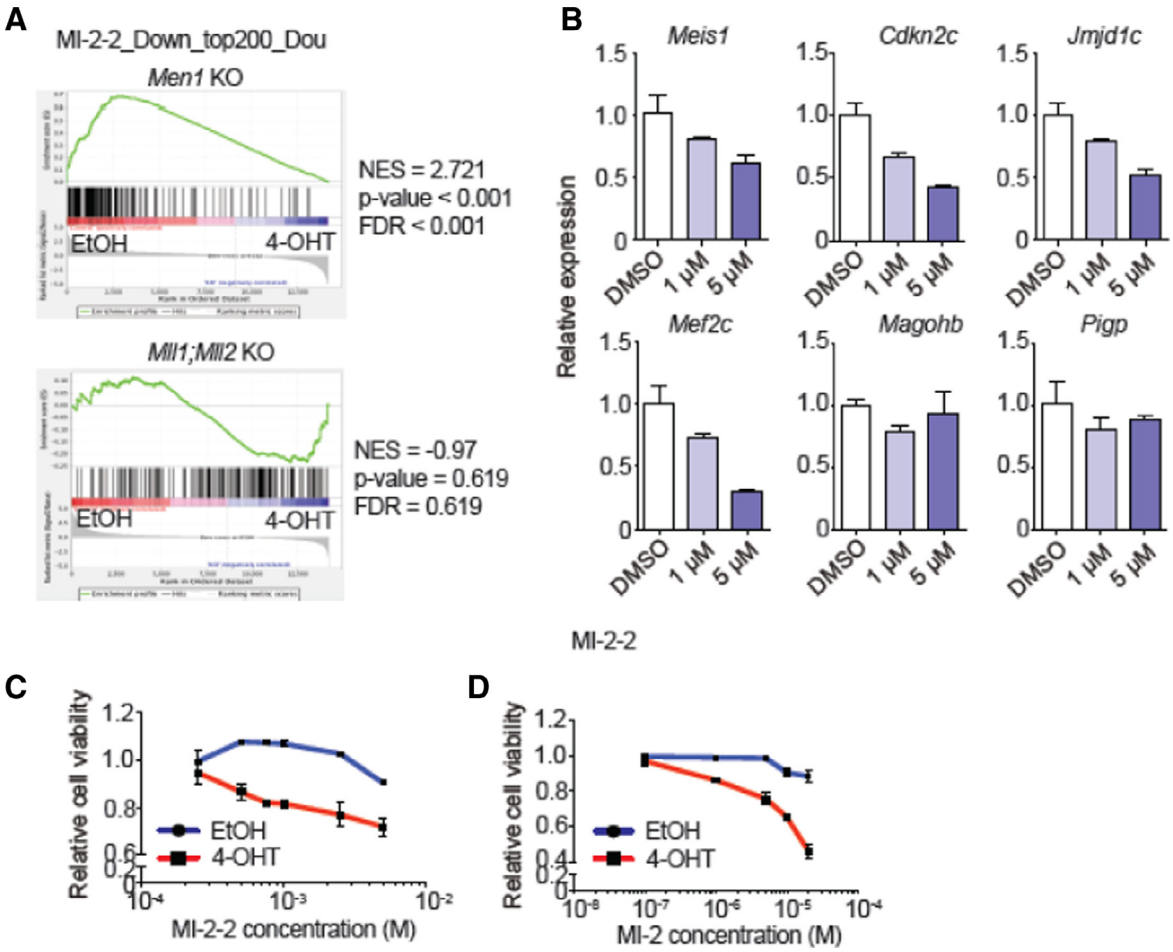

Figure 2. Menin inhibitors phenocopy *Men1* deletion and collaborate with *Mll1;Mll2* loss to kill leukemia cells. **(A)** GSEA plots showing enrichment of MI-2-2-regulated genes [20] in *Men1*-deleted MLL-AF9 cells and in *Mll1;Mll2*-deleted MLL-AF9 cells. **(B)** qRT-PCR of selected target genes after MI-2-2 treatment in MLL-AF9-transformed cells. Gene expression was determined 72 hours after treatment. Data are represented as averages ± standard deviation (SD). **(C,D)** Relative cell viability after and MI-2-2 **(C)** and MI-2 **(D)** treatment in MLL-AF9-transformed cells with or without *Mll1;Mll2*. MLL-AF9-transformed cells with the genotype of $Cre^{+};Mll1^{F/F};Mll2^{F/F}$ were treated with ethanol or 4-OHT for 24 hours, washed, and then treated with compound or vehicle for 3 additional days. Cell viabilities were all normalized to the corresponding vehicle (ethanol) control. Data are represented as mean ± SD. One representative experiment of two is shown.

were significantly and reproducibly downregulated upon *Men1* deletion, as was the menin-regulated gene *Cdkn2c*/p18, whereas expression of these genes changed minimally or not at all upon *Mll1;Mll2* deletion (Figure 1E and Chen et al. [12]). In contrast, the MLL2-regulated genes *Magohb, Pigp*, and *Il3ra* were downregulated by *Mll1;Mll2* deletion and not *Men1* deletion (Figure 1E). *Men1* deletion specifically reduced the expression of MLL-AF9-bound, MLL-AF9 upregulated, and Dot1L-dependent genes, consistent with its role as a requisite binding partner of MLL-FPs (Figure 1F). In contrast, *Mll1;Mll2* deletion did not significantly affect the same gene sets (Figure 2A). These results illustrate that *Men1* deletion specifically affects MLL-FP activity rather than the combined activity of MLL-FPs and endogenous MLL1/MLL2 [15,16]. Although loss of MLL1/MLL2 effectively kills MLL-AF9 cells, it apparently does so through distinct mechanisms and pathways compared with *Men1* deletion. MLL-FPs lack the C-terminal chromatin-targeting motifs of wild-type MLL1 and MLL2 [17–19], which may result in a stronger dependency on the N-terminal menin-LEDGF complex than wild-type MLL1 or MLL2.

Because menin and MLL1/MLL2 regulate distinct pathways, we hypothesized that *Mll1;Mll2* co-deletion would be complementary to inhibition of the menin–MLL-FP interaction. Therefore, we tested the combined effect of *Mll1;Mll2* deletion with the menin–MLL1 small-molecule inhibitor MI-2 and its higher-affinity variant MI-2-2 [9,10]. Comparing *Men1* deletion with the previously described effect of MI-2-2 on

murine MLL-AF9 cells [20], MI-2-2-downregulated genes were significantly enriched in our *Men1*$^{-/-}$ AML data using GSEA (Normalized Enrichment Score [NES] >2.7, $p < 0.001$), whereas *Mll1;Mll2* double-knockout genes were not (NES <1.5, $p > 0.1$; Figure 2A). Validation experiments using independently transformed MLL-AF9 cells showed that MI-2-2 inhibited expression of the direct MLL-FP target genes *Meis1, Cdkn2c, Jmjd1c*, and *Mef2c*, but not MLL2 target genes (Figure 2B). We therefore tested the sensitivity of *Mll1;Mll2*-deleted, MLL-AF9-transformed cells to menin inhibitors relative to the parental cells to determine whether inhibition of both pathways provided additional cell killing. Strikingly, *Mll1;Mll2*-deficient MLL-AF9-transformed cells showed a more than 10-fold increased sensitivity to both MI-2 and MI-2-2 (Figures 2C and 2D) [9,10]. Therefore, combined inhibition of menin and MLL1/MLL2 more effectively kills *MLL*-rearranged leukemia cells, likely due to their effects on distinct genetic networks. These data also predict that targeting MLL1/MLL2 in combination with other MLL-FP-directed strategies (e.g., DOT1L inhibitors) may result in synergistic killing of leukemia cells, similar to the demonstration that targeting MLL-FPs with two different molecular inhibitors can produce synergistic effects [21].

The observation that MLL-FPs are much more strongly dependent upon menin genetically or upon menin interaction (based on use of MI-2-2) demonstrates an interesting and perhaps unanticipated gained dependency by the fusion oncoprotein. This phenomenon may be attributed to the distinct multivalent chromatin interactions between MLL1 and is fusion oncoprotein derivatives, which may also be related to the observed spreading of both MLL-FPs and menin into gene bodies in MLL-FP-expressing cell lines [14,22]. Our data begin to unravel the nature of this gained dependency, but further molecular characterization will be required to completely understand the basis for the apparently selective effect of menin inhibitors on MLL-FPs and how menin inhibition can be combined with additional strategies to maximize the specificity and selectivity of its antileukemia activity.

Acknowledgments

We thank Kathrin Bernt for critical comments and our laboratory members for discussion and critical comments.

This work was sup ported by grants from the National Institutes of Health (HL090036 and CA224436 to PE and CA046934 and CA160467 to JG).

YC performed most experiments and collected and analyzed data. YC and PE designed the experiments, interpreted data, and wrote the manuscript. YC and KLJ analyzed the RNA-seq data. MM, KA, AK, and AFS generated essential animal models. JG developed and provided the MI-2-2 compound.

Conflict of interest disclosure

PE owns Amgen stock and has consulted for Servier Oncology. JG receives research support, has equity ownership in, and consults for Kura Oncology, Inc. YC is employed by Seattle Genetics, Inc. The remaining authors declare no competing financial interests.

References

1. Pui CH, Yang JJ, Hunger SP, et al. Childhood acute lymphoblastic leukemia: progress through collaboration. J Clin Oncol. 2015;33:2938–2948.
2. Yokoyama A, Somervaille TC, Smith KS, Rozenblatt-Rosen O, Meyerson M, Cleary ML. The menin tumor suppressor protein is an essential oncogenic cofactor for MLL-associated leukemogenesis. Cell. 2005;123:207–218.
3. Zhu L, Li Q, Wong SH, et al. ASH1L links histone H3 lysine 36 dimethylation to MLL leukemia. Cancer Discov. 2016;6:770–783.
4. Hughes CM, Rozenblatt-Rosen O, Milne TA, et al. menin associates with a trithorax family histone methyltransferase complex and with the hoxc8 locus. Mol Cell. 2004;13:587–597.
5. Milne TA, Briggs SD, Brock HW, et al. MLL targets SET domain methyltransferase activity to Hox gene promoters. Mol Cell. 2002;10:1107–1117.
6. van Nuland R, Smits AH, Pallaki P, Jansen PW, Vermeulen M, Timmers HT. Quantitative dissection and stoichiometry determination of the human SET1/MLL histone methyltransferase complexes. Mol Cell Biol. 2013;33:2067–2077.
7. Murai MJ, Pollock J, He S, et al. The same site on the integrase-binding domain of lens epithelium-derived growth factor is a therapeutic target for MLL leukemia and HIV. Blood. 2014;124:3730–3737.
8. Borkin D, He S, Miao H, et al. Pharmacologic inhibition of the menin-MLL interaction blocks progression of MLL leukemia in vivo. Cancer Cell. 2015;27:589–602.
9. Grembecka J, He S, Shi A, et al. menin−MLL inhibitors reverse oncogenic activity of MLL fusion proteins in leukemia. Nat Chem Biol. 2012;8:277–284.
10. Shi A, Murai MJ, He S, et al. Structural insights into inhibition of the bivalent menin−MLL interaction by small molecules in leukemia. Blood. 2012;120:4461–4469.
11. Xu S, Aguilar A, Xu T, et al. Design of the first-in-class, highly potent irreversible inhibitor targeting the menin−MLL protein −protein interaction. Angew Chem Int Ed Engl. 2018;57:1601–1605.
12. Chen Y, Anastassiadis K, Kranz A, et al. MLL2, not MLL1, plays a major role in sustaining MLL-rearranged acute myeloid leukemia. Cancer Cell. 2017;31:755–770.
13. Hulsen T, de Vlieg J, Alkema W. BioVenn: a web application for the comparison and visualization of biological lists using area-proportional Venn diagrams. BMC Genomics. 2008;9:488.
14. Kerry J, Godfrey L, Repapi E, et al. MLL-AF4 spreading identifies binding sites that are distinct from super-enhancers and that govern sensitivity to DOT1L inhibition in leukemia. Cell Rep. 2017;18:482–495.
15. Zuber J, Rappaport AR, Luo W, et al. An integrated approach to dissecting oncogene addiction implicates a Myb-coordinated self-renewal program as essential for leukemia maintenance. Genes Dev. 2011;25:1628–1640.
16. Bernt KM, Zhu N, Sinha AU, et al. MLL-rearranged leukemia is dependent on aberrant H3K79 methylation by DOT1L. Cancer Cell. 2011;20:66–78.

17. Ali M, Hom RA, Blakeslee W, Ikenouye L, Kutateladze TG. Diverse functions of PHD fingers of the MLL/KMT2 subfamily. Biochim Biophys Acta. 2014;1843:366–371.
18. Milne TA, Kim J, Wang GG, et al. Multiple interactions recruit MLL1 and MLL1 fusion proteins to the HOXA9 locus in leukemogenesis. Mol Cell. 2010;38:853–863.
19. Couture JF, Collazo E, Trievel RC. Molecular recognition of histone H3 by the WD40 protein WDR5. Nat Struct Mol Biol. 2006;13:698–703.
20. Xu J, Li L, Xiong J, et al. MLL1 and MLL1 fusion proteins have distinct functions in regulating leukemic transcription program. Cell Discov. 2016;2:16008.
21. Dafflon C, Craig VJ, Méreau H, et al. Complementary activities of DOT1L and menin inhibitors in MLL-rearranged leukemia. Leukemia. 2017;31:1269–1277.
22. Ruthenburg AJ, Li H, Patel DJ, Allis CD. Multivalent engagement of chromatin modifications by linked binding modules. Nat Rev Mol Cell Biol. 2007;8:983–994.